LBL-16565
Preprint c.2

Lawrence Berkeley Laboratory
UNIVERSITY OF CALIFORNIA

Accelerator & Fusion Research Division

Submitted to Nuclear Instruments and Methods

RECEIVED
1983
LBL LIBRARY

THE LBL EBIS TEST STAND

I.G. Brown and B. Feinberg

September 1983

TWO-WEEK LOAN COPY
This is a Library Circulating Copy which may be borrowed for two weeks. For a personal retention copy, call Tech. Info. Division, Ext. 6782.

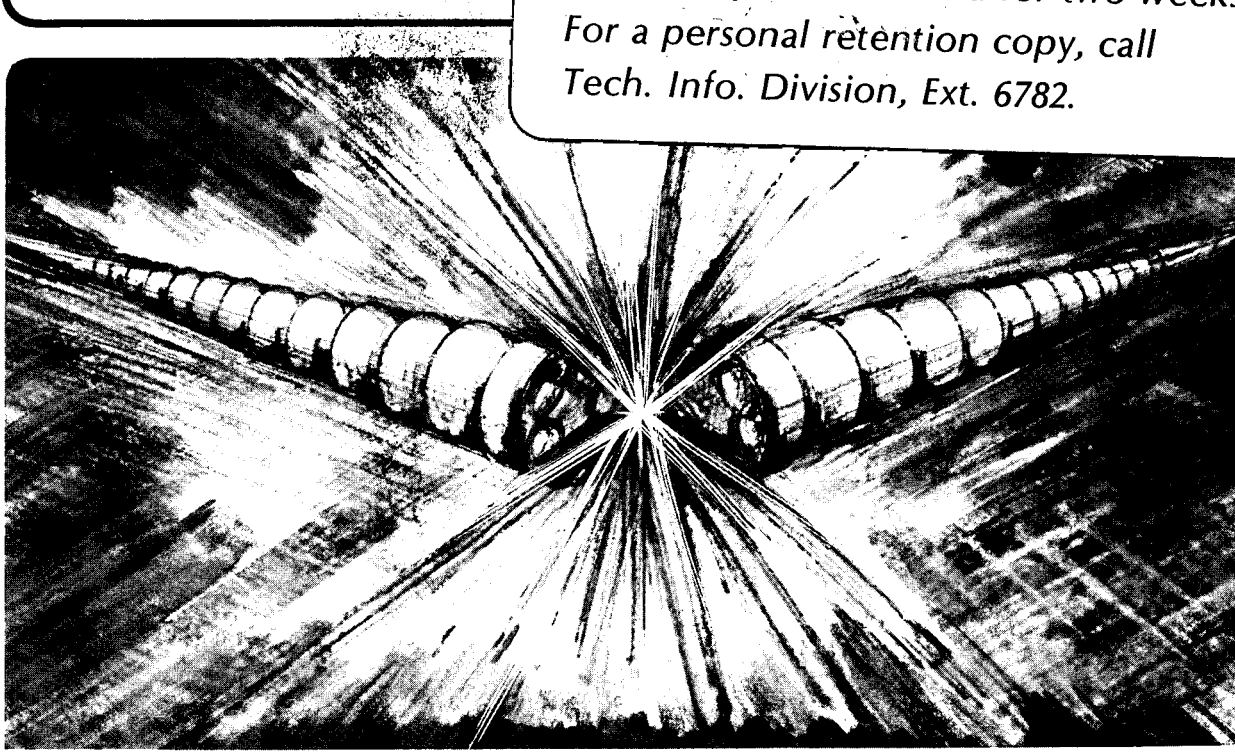

LBL-16565 c.2

Prepared for the U.S. Department of Energy under Contract DE-AC03-76SF00098

DISCLAIMER

This document was prepared as an account of work sponsored by the United States Government. While this document is believed to contain correct information, neither the United States Government nor any agency thereof, nor the Regents of the University of California, nor any of their employees, makes any warranty, express or implied, or assumes any legal responsibility for the accuracy, completeness, or usefulness of any information, apparatus, product, or process disclosed, or represents that its use would not infringe privately owned rights. Reference herein to any specific commercial product, process, or service by its trade name, trademark, manufacturer, or otherwise, does not necessarily constitute or imply its endorsement, recommendation, or favoring by the United States Government or any agency thereof, or the Regents of the University of California. The views and opinions of authors expressed herein do not necessarily state or reflect those of the United States Government or any agency thereof or the Regents of the University of California.

LBL-16565

The LBL EBIS Test Stand

I.G. Brown and B. Feinberg

Lawrence Berkeley Laboratory
University of California
Berkeley, California 94720

September 1983

This work was supported by the Director, Office of Energy Research, Office of High Energy and Nuclear Physics, Nuclear Physics Division, of the U.S. Department of Energy under Contract Number DE-AC03-76SF00098.

The LBL EBIS Test Stand

I. G. Brown and B. Feinberg

Abstract

An Electron Beam Ion Source test stand has been constructed to investigate the characteristics of EBIS operation important to reliable application as a cyclotron ion source. Ion output scaled as expected with containment length, beam current, and magnetic field, and there were indications of slight beam collapse needed for high duty cycle operation. Impurity gas problems indicate the need for cryogenic pumping in a full scale source. Reliability and reproducibility, both short and long term, were excellent.

---

*This work was supported by the Director, Office of Energy Research, Office of High Energy and Nuclear Physics, Nuclear Physics Division, of the U.S. Department of Energy under Contract No. DE-AC03-76SF00098.

I. Introduction

Considerable interest has developed in recent years in the EBIS - Electron Beam Ion Source - as a source of highly stripped heavy ions for injection into particle accelerators, and for atomic physics research. Ion species as highly stripped as Xe^{52+} have been observed[1] with particle production rates of around 10^7 particles/pulse of that species. The ion energy output by a circular accelerator is given in the non-relativistic approximation by $E/A = KQ^2/A^2$, where Q is the charge state of the ion (electron units) and A its mass (amu); thus increasing the charge state of the ion provides a convenient means of upgrading the performance of an existing accelerator. Also, the need is growing to make basic cross-section measurements for various highly stripped heavy ion interactions for controlled fusion research; the fusion plasma environment contains such species as impurities, and prediction of the plasma behavior and energy balance requires a knowledge of these cross-sections. A laboratory-sized EBIS facility is thus of interest to the fusion and atomic physics communities also.

In the EBIS, a high density electron beam is used to ionize a batch of ions in a straight magnetic field. The ions are confined radially by the space charge field of the electron beam itself and axially by the electrostatic potential well established by voltages applied to a set of cylindrical metal tubes (the drift tubes) surrounding the beam (see figure 1). Feed material - the atomic species to be ionized - is injected into the beam and is ionized by successive electron impact to a maximum charge state determined by the electron beam current density, the

ion residence time within the beam, and the background gas pressure. When this maximum degree of ionization is obtained, the axial potential distribution is changed from ion confinement to ion expulsion, and the ions are extracted and steered into the accelerator or experimental chamber. The cycle is then repeated.

Our aim was to construct a small EBIS test stand to investigate EBIS operation and to identify those characteristics that are particularly important to reliable application of the EBIS as a cyclotron ion source (as opposed to synchrotron or other). Our device is named BEBIS - the Berkeley EBIS. In this paper the BEBIS device is described along with the results obtained using it.

II. Operating Principles

The multiple ionization of positive ions by successive electron impact is a well known phenomenon. For maximum ionization, the ions should be confined within the stripping region (i.e., the electron beam) for times that are sufficiently long for the trapped ions to be repeatedly struck by ionizing electrons. With this philosophy, Redhead[2] made use of both a magnetic field to confine the electron beam and externally applied potentials to confine the positive ions. Donets[3] and the Dubna group added the features of extremely high vacuum, of operation in a pulsed mode so as to trap the ions until they are maximally stripped, and of injecting the electron beam into the magnetic field from a high quality electron gun so as to produce a high density electron beam, and thereby created what has become known as the EBIS. In the ensuing 15 years EBIS development has been continued by workers at a number of laboratories[4], most notably by Donets et al. at Dubna[5] and by Arianer et al. at Orsay[6].

Consider an electron beam of energy V_b and current density J within which a background of positive ions resides. Ionization takes place via a stepwise process, the characteristic time τ_i for each step of ionization from charge state i-1 to i being given by $\tau_i = e/J\sigma_i$, where e is the electronic charge, J, the electron beam current density, and σ_i, the cross-section for ionization from a state of charge i-1 to i. Thus the total time needed to arrive at a charge state Z from the neutral atom state is

$$\tau_Z = \frac{e}{J} \sum_{i=1}^{Z} \frac{1}{\sigma_i} \quad . \tag{1}$$

This is dominated by the final step from charge state Z-1 to Z, and for a first estimate it is adequate[7] to make the approximation

$$\tau_Z = \frac{e}{J\sigma_Z} \tag{2}$$

The cross-section σ_Z can be approximated by the semi-empirical formula of Lotz[8] for ionization by single electron impact from charge state Z-1 (ground state) to charge state Z,

$$\sigma_Z \simeq 4.5 \times 10^{-20} \frac{\ln(V_b/\Phi_Z)N_Z}{V_b\Phi_Z} \ (\mathrm{cm}^2) \quad . \tag{3}$$

where V_b is the electron beam voltage (kV), Φ_Z is the ionization potential (in keV) from the ground state of ionization Z-1 to Z, and N_Z is the number of electrons in the outer subshell of Z-1. Combining equations (2) and (3) and putting $V_b \sim 20$ kV, one obtains the condition

$$J\tau \sim 10^5 - 10^6 \ (\mathrm{A/cm}^2)(\mathrm{msec}) \tag{4}$$

for species like Xe^{44+}. This product, $J\tau$, is of basic importance to EBIS operation; it determines the maximum charge state obtained, assuming that the electron beam voltage is not a limitation. For confinement times as short as 10 msec, needed for high duty cycle operation, the beam current density must approach the very high value ~ 100 kA/cm^2 to produce (e.g.) Xe^{44+}.

The background vacuum quality is important from two separate points of view: (a) the beam should be loaded with the wanted feed material ions and not with ions from the background gas; (b) charge exchange of highly stripped ions with the background gas should not limit the attainable charge state. Normally the first condition is a more severe vacuum requirement than is the second. One requires that the background gas atoms, which in a clean system will be principally hydrogen, load the beam no more than, say, 10% of capacity (when the ion charge in the beam equals the electron charge and the beam is thus fully neutralized) during the maximum confinement time of about 10 msec. Thus one has

$$Q_i = 0.1\ Q_e \tag{5}$$

where Q_i is the (hydrogen) background gas ion charge within the beam of length L and cross-sectional area A, and Q_e is the electron charge in the same region. Noting that

$$\frac{dn_i}{dt} = n_o\ n_e\ \sigma_i\ v_e \tag{6}$$

equation (5) becomes

$$n_o\ n_e\ \sigma_i\ v_e\ eAL\ \tau_i = 0.1\ n_e\ eAL$$

or

$$n_o = (10\sigma_i \; v_e \; \tau_i)^{-1} \quad , \tag{7}$$

where n_o is the background gas atom density, n_e the beam electron density, n_i the density of background gas ions within the beam, σ_i the ionization cross-section, v_e the beam electron velocity and τ_i the confinement time of interest. For a several kV electron beam, and taking $\sigma_i \sim 4 \times 10^{-18}$ cm^2 and $\tau_i \sim 10$ msec, one obtains the condition

$$P < 10^{-8} \text{ Torr.} \tag{8}$$

These requirements, together with other aspects of the physics of EBIS, are discussed in some depth by Vella[7]. The conditions (4) and (8) along with the beam voltage really define the EBIS, given the assumption that the electron beam and ion background cross sectional areas coincide. Further requirements on the device are essentially just requirements for achieving these conditions.

Thus the electron beam current density needed is $\sim 10^5$ Amps/cm^2. The maximum current density that can be obtained from a gun operating at around 10 kV is several amperes, due to the perveance limit of several micropervs (1 perv = 1 Amp/Volt$^{3/2}$) for practical guns. If the gun is magnetically well shielded, so that the field on the cathode is essentially zero (say < 1 G) and the beam is properly injected into a spatially rising magnetic field of strength the order of one Tesla, one can obtain current densities from several hundred to perhaps $\sim 10^3$ Amps/cm^2. A further increase in current density by a factor $\sim 10^2$ is thus needed. From another perspective, one can conclude that those experiments[9] that have produced results similar to the example above

(Xe^{44+} in $\lesssim$ 10 msec) imply a beam current density two orders of magnitude higher than the "bare beam" current density. An hypothetical explanation for this beam compression is the collapse of the beam due to electron space charge neutralization. The bare beam, if properly matched to the magnetic field and in Brillouin flow[10], rotates about its axis (at one half the electron cyclotron frequency, $\omega = 1/2\ \omega_{ce}$) due to the E x B interaction between the radial electrostatic field and the axial magnetic field; the beam is then in rotational equilibrium between the centrifugal and space charge forces radially outwards and the v x B force inwards. As the beam becomes loaded with positive ions, the net charge of the beam approaches zero and so also the radial electrostatic field supporting the beam outwards. The beam thus collapses upon itself and the current density becomes very high, limited by the departure from ideal Brillouin flow in the bare beam. This phenomenon of beam neutralization and collapse can be central to EBIS operation for the case when the electron gun is operated as an 'external gun' - i.e., with the gun cathode well shielded from the magnetic field and the field on the cathode $B_K = 0$. Note that alternative modes of operation are for the gun to operate semi-immersed ($0 < B_K < B_o$) or immersed ($B_K = B_o$). For a semi-immersed gun the beam geometric compression in the magnetic field will be less, and obtaining a sufficient $J\tau$ product is achieved by increasing τ; this in turn necessitates a background gas pressure that is lower by at least a similar factor. The Dubna device, KRION II, operates in this mode - the gun is semi-immersed, the confinement time is about 2 seconds, and the background gas pressure is ~ 10^{-12} Torr. This mode of operation precludes cyclotron application, where high duty cycle is required.

III. Description of Device

The decade of experience gained by the various EBIS groups[4,5,6] in the 1970's has helped us immeasurably in our program. We were able to include in our thinking, from the outset, the problems and pitfalls that were painfully learned by others. Many of the features incorporated into our device are the result of our interaction with other groups, and we are indebted to these researchers for the open way in which they shared their EBIS experiences with us.

A schematic of BEBIS is shown in Fig. 2, and a photograph in Fig. 3. The device was designed to be as simple and inexpensive as possible, and to allow maximum flexibility for changes and for EBIS research and development. In this spirit, a normal conducting magnet (i.e., not super- conducting) and non-cryogenically cooled drift tubes were chosen. Nevertheless - and to a certain extent because of this - high vacuum quality, with a base pressure in the low 10^{-9} Torr range or better was desired. The vacuum vessel is 30 cm in diameter and 1.6 mm in wall thickness. Type 304 stainless steel (20% Cr, 12% Ni) is used throughout except for the 1m long section under the magnetic field coils where the drift tubes are located and the field quality is especially important. Type 310 stainless steel (26% Cr, 22% Ni) is used there because of the considerably lower magnetic susceptibility of type 310 and hence also the perturbation to the magnetic field. The system is all metal and OFHC (oxygen free, high conductivity) copper gaskets are used throughout, except for the nickel plated iron polepiece which is sealed to the stainless steel vacuum vessel using aluminum gaskets. Rough vacuum is produced by two liquid nitrogen cooled sorption pumps, and high vacuum by two 500 l/sec

ion pumps and a 1000 l/sec refrigerated helium cryopump. After an opening to air (or more correctly, to dry nitrogen) the entire vessel is baked to ~ 150°C for several days. Base pressure after baking is ~ 7×10^{-10} Torr.

Our electron gun is a Hughes 112-2B, manufactured by Hughes Electron Dynamics Division. This gun has a 7 mm diameter sintered tungsten cathode and a nominal perveance of 2.0 μp; maximum operating voltage is about 6 kV. The gun is mounted in a structure which allows it to be moved axially, in the transverse plane, and in tilt by means of 9 micrometer adjustable vacuum feedthroughs. In this manner the gun can be precisely aligned while at high vacuum.

There are 15 drift tubes plus the electron collector, and these 16 elements are supported within a structure in such a manner as to minimize changes in alignment due to thermal creep. A photograph of the drift tubes assembly is shown in Fig. 4. The drift tubes are aligned to be coaxial to within less than 25 μm. The drift tubes and support structure were fabricated of OFHC copper, and the entire assembly was vacuum baked at ~ 500°C for several days prior to installation in the device. This vacuum bake removes the hydrogen that is in solution in the OFHC copper; in fact the base pressure attainable in the device improved by a factor of two in this manner. The entire assembly - drift tubes, electron collector and support structure - is itself supported on non-magnetic, adjustable vacuum feedthroughs, so that the geometric axis of the drift tubes can be aligned while at high vacuum. There is at the far end of the machine (the ion extraction and analysis end) a window through

which the position in the transverse plane of the various elements can be accurately measured by means of a measuring telescope; the cathode of the gun provides good illumination for this purpose.

The magnetic field is established by three modular coils, each made of 144 turns of 1.27 cm square copper conductor, 41 cm ID, 71 cm OD, and 15 cm thick. The coils are water cooled (0.64 cm hole in the square conductor) and are powered by a 360 kW (maximum) DC motor generator set. The field magnitude can be varied up to 7 KG; for fields higher than this the iron that is used to shield the electron gun starts to saturate and the field to penetrate. An important requirement for good EBIS operation is that the magnetic field on axis be straight. That is, the field line that passes through the center of the electron beam entrance aperture should be straight, over the length of the drift tubes structure, to better than about 0.1 mm[11]. It has been usual in the past to meet this requirement by winding the solenoid very accurately using small diameter superconducting wire. Our approach has been to make use of existing coils within the laboratory that are by no means precision wound, and a structure of accurately machined and positioned (25 μm) soft iron rings. The iron ring structure acts as a 'magnetic field homogenizer' in that it determines the field shape rather than the copper coils; one can think of the current in the copper as energizing the iron and the precise tolerance of the homogenizer structure as determining the field quality. The homogenizer strucuture can be moved in position and in tilt as a single unit, and by this means the magnetic axis can be moved also. The design and operation of the homogenizer is described in detail in a separate publication[12].

The 3 coil solenoid is terminated at either end with a 7 cm thick disc of soft, well annealed iron. At the ion extractor end of the solenoid (exit end) a single bucking coil is mounted so as to trim the field shape in the region of the electron beam collector and ion extractor; this coil is driven by a separate power supply. The electron gun is housed in a cavity within the iron disc at the entrance end of the solenoid. The gun is operated as an external gun - that is with the gun cathode located in a zero-magnetic-field region. To achieve this condition it has been usual in the past to magnetically shield the gun as much as possible and tune to $B_k = 0$ using a small bucking coil surrounding the gun. By serendipity, the necessity of a gun bucking coil was avoided and instead the hysteresis in the iron polepiece and gun housing was used. Operationally, one simply approaches the desired main field strength via a pre-determined path and the required B_k ensues; this principal is indicated in Fig. 5.

Injection of feed material into the electron beam is a pivotal consideration. One has the conflicting requirements of relatively high pressure ($\sim 10^{-7}$ Torr) so that ionization and trapping within the beam will occur, and simultaneously a relatively low pressure ($\sim 10^{-9}$ Torr) within the ion confinement region so as to minimize charge exchange. One way in which these conditions can be met, and which has been used in other devices, is to cryogenically cool the drift tubes to near liquid helium temperature and to bleed in a noble gas (other than helium). A fraction of the gas is ionized by the electron beam and the vast majority is pumped by the cold drift tube interior surfaces. Since, for

simplicity, cryogenic drift tubes have been avoided, this technique cannot be used here. Instead, a number of material injection methods have been investigated:

1. Steady gas feed. The simplest method is to simply bleed in gas through a variable leak valve so as to raise the background pressure to a predetermined level. BEBIS was operated in this way with nitrogen and argon.
2. Calcium atomic oven. A small atomic oven was constructed which sprayed a sheet jet of calcium vapor through a 4 cm long, 1 mm wide, slot in a drift tube (drift tube number two) and thus through the electron beam. As a variant of this, the oven was positioned to spray vapor into the electron collector through a small hole in it, so as to coat some of the inside surface with a layer of calcium which could then be desorbed by the electron beam.
3. Laser evaporation. A surface of pure manganese metal was positioned outside a drift tube (number 9) in such a manner that it could be zapped by a pulsed ruby laser; the evaporated material would enter the drift tube and electron beam. A small filament was added so that the manganese target could be heated to incandescence in situ, to outgas it.
4. Gas puff injection. Finally, a commercially available (Veeco PV-10) piezo-electric gas puff valve was modified and mounted immediately adjacent to a drift tube, so as to admit a ~1 msec puff of gas into drift tube number 10. In this case, as also in the laser injection method, the two drift tubes on either side of the gas injection drift tube were 'opened up' so that gas could be pumped out of them into the main chamber.

Following the electron collector is the ion extractor and then the ion focussing and steering optics. Ions are detected at the far end of the time-of-flight chamber, a 2-meter extension to the main chamber. The detector was either a gridded Faraday cup or an electron multiplier structure.

IV. Device Operation

In this section we describe the results of various measurements on our EBIS test-stand magnetic field quality, electron beam quality, injection systems, ion output, scaling laws, and reproducibility.

1. Magnetic Field

The on-axis magnetic field shape, $B_z(z)$, is shown in Figure 6. The field is fairly flat in the trapping region, which results in a constant electron beam size and hence also a constant space charge potential. Thus the field uniformity makes it unnecessary to individually adjust the drift tube potentials in the trap. At the exit of the device, precise control over the field fall-off and field null is provided by a bucking coil. This is essential to assure that the electron beam is well 'aimed' and dumps into the water-cooled electron collector rather than elsewhere. Measurements of the magnetic field straightness have been reported previously[12], and data from a typical measurement are shown in Figure 7a. This is a plot of the projection in the transverse plane of a field line trajectory located nearly on axis. The field is straight to within ±40 μm over the axial distance of 60 cm, well within the sought tolerance of ±100 μm.

2. Electron Beam

The electron beam trajectory has been measured by observing with a measuring telescope the 'bright-up' produced when the pulsed (~ 10 μsec pulses, ~ 10 pulses per second) electron beam stikes a witness plate (25 μm thick tungsten foil) which is progressively moved along the axis of the vessel. These measurements have been reported previously also[12]. Again, the trajectory was found to be straight to better than ±40 μm (see Figure 7b).

An extensive series of measurements of the current profile of the bare electron beam was carried out. A multiwire probe, built for these measurements, consists of 14 vertical tungsten wires, 25 μm diameter and spaced 50 μm between centers, along with 14 similar horizontal wires located about 1 mm behind the vertical wires. The probe can be postioned accurately in the transverse plane by means of the micrometer adjustable vacuum feedthroughs that otherwise support the drift tubes assembly, and it is also moveable in the axial direction. The electron beam is pulsed (~ 10 μsec) in order to avoid melting the wires, and the current to each wire is monitored using our computer data-acquisition system.

The profile so obtained, which is a plot of the current to various chords, is displayed immediately following the shot. An Abel inversion routine[13], programmed into the computer, allows this data to be unfolded into the wanted radial profile of current density, J(r). Figure 8 shows an example of typical raw data and current profile.

Matching of the electron beam to the magnetic field is important; i.e., the transition from electrostatically dominated flow within the gun region, up to the focus of the electron beam, to magnetically dominated flow along the magnetic field must be made carefully. A good match will allow high current density, both for the bare beam and for the collapsed external beam. A mismatch will lower the bare beam current density, and can also limit the maximum beam compression, due to space charge neutralization, that can be obtained. Figure 9a shows the current density, J, averaged over the FWHM, as a function of gun voltage; Figure 9b shows similar data for J versus the magnetic field strength. For conditions typical of our operating regime, the bare beam current density is around 100 Amps/cm^2, up to a maximum of about 200 Amps/cm^2. The current density rises approximately linearly with the magnetic field strength. This behavior is to be expected when using a high perveance gun since beam aberrations grow rapidly with perveance.[14] For an ideal electron gun the current density would be proportional to magnetic field strength squared.[14] These data were taken at a fixed axial location, $z \simeq 20$ cm. A series of measurements of beam profile evolution as a function of distance from the gun has also been taken, and an example of such data is shown in Figure 10. The main conclusion to be drawn from these J(r,z) data is that near the optimum gun voltage the beam profile indeed shows little axial variation.

3. Injection Systems

The steady gas feed method was used extensively and all of the scaling results were obtained with this type of injection. There is a major limitation with this method, however. New ions are continually created from the background gas fed in, so the gas acts as a source of low charge state ions. At any desired expulsion time there are ions in the well which have only just entered, and are therefore not stripped to the extent they would be if they had been confined for the entire containment time. This effect lowers the average charge state, and, since the well has a finite capacity, reduces the quantity of high charge state ions expelled.

The calcium atomic oven and the laser evaporation methods were relatively unsuccessful. It was very difficult to sufficiently outgas the oven. Since gas can pass through the beam many times, while the calcium sticks to the walls, outgassing is critical. Outgassing the target for the laser evaporation injection was more successful. Heating the target by electron bombardment reduced the gas problem. The threshold for plasma production, however, was sufficiently close to the power needed to evaporate atoms that shorting out the drift tube potentials became a problem. While this could be somewhat rectified by lowering the voltages during the laser pulse, no charge states of manganese higher than Mn^{8+} were seen.

The gas puff injection system worked reasonably well. Charge states as high as Ar^{11+} were observed. The major problem with this method involved the low Curie point of the piezo-electric crystal in the puff valve, which made bake out of the system, and therefore reduction in background pressure, difficult.

4. Ion Charge State Output

A typical charge state spectrum of nitrogen, using the steady gas feed injection method is shown in Figure 11. By examining the ratio of adjacent peak heights one can determine the current density, solving the coupled ionization rate equations and using the Lotz cross sections.[8] The peak heights are divided by the charge state to get the quantity of ions, in qualitative agreement with a calibration of the electron multiplier. Comparison with this model, using spectra taken at a number of confinement times, implies a current density of $J \sim 240 \pm 50$ A/cm^2 for a 4 kV, 390 mA beam and a 3 kG field. Figure 9 shows that the bare beam current density, J, equals 150 ± 30 A/cm^2. Since the Lotz cross sections have only been verified within a factor of two[15], the increase in density cannot be taken as being a verification of beam collapse, although it may be suggestive. For conditions which appear to be less well matched, and therefore less susceptible to collapse, a 2.5 kV, 220 mA beam in a 3 kG field, the charge state distribution implies $J = 120 \pm 50$ A/cm^2 while the bare beam current density was found to be 110 A/cm^2, in better agreement.

Figure 12 shows a charge state spectrum of argon using the gas puff injection method. This oscillogram was taken before the system was thoroughly baked out, and therefore many impurity peaks are present. Analysis of the argon spectrum for this case, with a 2.5 kV, 190 mA beam and a 3 kG field, implies a current density $J = 140 \pm 10$ A/cm^2. Figure 9 shows the bare beam density to be 110 A/cm^2. These data indicate that some beam collapse may occur when the beam is optimally matched to the field.

5. EBIS Scaling

A major part of the experimental effort has been devoted to confirming the theoretical EBIS scaling. Our major interest is the number of ions produced in each experimental cycle, and the charge state distribution of those ions. Also of interest are any limitations on the repetition rate of the source, which is related to collector cooling, and any limitations on increasing the duration of the extraction pulse, both of which influence the duty cycle. All scaling measurements were made with the steady gas feed injection method.

The fundamental limit on the number of ions produced per pulse is due to space charge neutralization. The electron beam space charge provides the radial ion confinement, and thus the ion number is limited by

$$\sum_i Z_i N_i \leq N_e, \tag{9}$$

where Z_i is the ion charge state, N_i is the number of ions of charge state Z_i in the trapping region, and N_e is the number of beam electrons in the trapping region. The number of beam electrons is given by

$$N_e = \frac{I_e L}{e v_e} = \frac{I_e L}{e(2kV_e/m_e)^{1/2}} \tag{10}$$

where I_e is the electron beam current, L is the length of the trapping region, and v_e is the electron velocity. V_e, the electron energy, is $V_G + V_T$, where V_G is the gun voltage and V_T the drift tube voltage. The ion output for various combinations of drift tubes, i.e. trapping lengths, has been measured and the ion output per unit length is constant to within ±10%, i.e., N_i increases linearly with L as predicted. Figure 13 shows this scaling.

Since the electron gun operates in a space charge limited mode, the gun current is proportional to $V_G^{3/2}$. Changing the gun voltage also changes the electron velocity, which also depends on the drift tube potentials. The ion output for various gun voltages has been measured, and the results of such a measurment are shown in Figure 14a. The ion output is seen to increase with V_G as predicted, proportional to $V_G^{3/2}/(V_g + V_T)^{1/2}$, where $V_T = 3$ kV.

The scaling of total ion charge is predicted to be independent of the confining magnetic field strength B, since it is limited only by the space charge neutralization. A measurement of N_i as a function of B is shown in Figure 14b. As predicted, N_i is independent of B.

Implicit to the above measurements is the "loading efficiency" of the beam - the measured value of Q_i/Q_e, where Q_i is the total positive ion charge in the trapping region and Q_e is the total beam electron charge in the trapping region. A loading of 100% is the maximum possible, and occurs for full space charge neutralization. The scaling laws above show the expected dependencies of ion output (N_i or Q_i) on L, V_G and B, and the proportionality factor is a direct measure of the loading efficiency, through equations (9) and (10). This was measured to be 30 to 35%.

An important parameter for the use of an EBIS with an accelerator is the duty cycle. For cyclotron operation one would like to stretch the extracted ion pulse out in time from its "natural" width of about 30 μs to a time of the order of 5 ms. One would also like to increase the repetition rate up to about 50-100 pulses per second. Here, the repetition rate was increased from 1 pulse per second up to 30 pulses per second.

While there was no degradation of the nitrogen charge state distribution, the source became polluted with carbon, thus decreasing the amount of nitrogen extracted. These experiments were performed with a poorly pumped, uncooled electron collector. Since source pollution was the only observed effect, it is likely that better pumping and cooling of the collector would allow high repetition rates. The output pulse was strectched in time up to 5 ms, as shown in Figure 15. Examination of the charge state distribution at various times during the extraction pulse showed little change in the spectrum.

6. Reliability and Reproducibility

We have found the device output to be very consistent on both a short term and a long term basis, when the machine is properly "tuned up". Our procedure was to empirically adjust all voltages - drift tubes, extraction, steering and focusing - so as to maximize the detected ion output signal. When so adjusted, the shot-to-shot variation in both the total ion charge output and the time-of-flight charge state spectrum is minimal. Oscillograms showing a ten-shot overlay of each of these signals are shown in Figure 16; clearly, the reproducibility is excellent. Furthermore, the long-term reproducibility is good also - one can simply switch on the device after many weeks of not running, and good spectra will be obtained.

V. Conclusion

An electron beam ion source test stand, BEBIS, has been built to investigate scaling and reliability with reference to cyclotron injection. The results indicate that an EBIS can be a reliable ion source, and that the quantity of ions produced is in good accord with expected EBIS scaling. For cyclotron operation a high repetition rate is needed. This, together with the difficulties of various injection methods, indicates the need for a cryogenic pumping system in the containment region. The phenonmenon of beam "collapse", needed to get high charge states in a short time, has not been definitively demonstrated, although there are indications of a slight collapse under optimum conditions. The use of a more laminar electron gun optimized for EBIS operation could aid in achieving collapse.

Acknowledgments

We gratefully acknowledge the efforts of J. Galvin, R. Kopa, and R. Peterson in the design and assembly of the test stand, W. B. Kunkel and M. C. Vella for their aid and insight into EBIS operation, and K. Halbach for aid in the magnetic field design. A special thanks is due to W.I.B. Smith (deceased) for design and operation of the laser injection system.

References

1. E. D. Donets, Phys. Scripta T3 (1983) 11.
2. P. A. Redhead, Can. J. Phys. 45 (1967) 1791.
3. E. D. Donets, IEEE Trans. Nucl. Sci. NS-23 (1976) 897.
4. See, for example, IEEE Trans. Nucl. Sci., NS-23 (1976) p. 979-1030.
5. E. D. Donets, Fiz. Elem. Chastits At. Yadra 13 (1982) 941, in translation, E. D. Donets, Sov. J. Part. Nucl. 13 (1982) 387.
6. J. Arianer, A. Cabrespine, C. Godstein, Nucl. Instr. and Meth. 193 (1982) 401 and J. Arianer, A. Cabrespine, C. Goldstein, T. Junquera, A. Courtois, G. Deschamps, M. Oliver, Nucl. Instr. and Meth. 198 (1982) 175.
7. M. C. Vella, Nucl. Instr. and Meth. 187 (1981) 313.
8. W. Lotz, Zeits. fur Phys. 216 (1968) 241.
9. J. Arianer, A. Cabrespine, C. Goldstein, IEEE Trans. Nucl. Sci. NS-26 (1979) 3713.
10. See, for example, P. Kirstein, G. Kino, W. Waters, "Space Charge Flow", (McGraw Hill, New York, 1967), p. 153ff.
11. J. Arianer, private communication.
12. B. Feinberg, I. G. Brown, K. Halbach, W. B. Kunkel, Nucl. Instr. and Meth. 203 (1982) 81.
13. K. Bockasten, J. Opt. Soc. Amer. 51 (1961) 943.
14. See Ref. 9, p. 194ff.
15. E. D. Donets, V. P. Ovsyannikov, V. G. Dudnikov, Comm. of the Joint Inst. for Nucl. Res., P7-12905, Dubna, USSR (1979).

Figure Captions

Figure 1. a) EBIS schematic showing the electron gun and collector, the drift tubes, and the solenoid.

b) Drift tube axial potential distributions for injection, trapping, and expulsion.

Figure 2. Schematic of the BEBIS test stand.

Figure 3. Photograph of the BEBIS test stand.

Figure 4. Photograph of the drift tubes and support structure.

Figure 5. Hysteresis curves showing the magnetic field at the cathode (B_k) versus the main solenoid field (B_0). The cathode field can be set equal to zero by following the appropriate curve.

Figure 6. Magnetic field strength along the axis.

Figure 7. a) Projection in the transverse plane of the axial magnetic field line. The points are positions along the axis, measured in centimeters from the polepiece near the electron gun.

b) Projection in the transverse plane of the electron beam trajectory.

Figure 8. Electron beam current profile.

a) Raw data showing the current to each wire chord versus position.

b) Abel inverted current density versus radius.

Figure 9. a) Current density as a function of cathode voltage, measured 20 centimeters from the polepiece.

b) Current density as a function of magnetic field, measured 20 centimeters from the polepiece.

Figure 10. Current to each wire chord for various axial positions near the polepiece.

Figure 11. Time of flight charge state analysis for nitrogen. V_k = 2.5 kV, B = 3.0 kG, and the confinement time, τ_c= 2 ms.

Figure 12. Time of flight charge state analysis for argon. Upper trace: background gas, τ_c = 4 ms. Lower trace: 3 ms gas puff of argon, τ_c = 4 ms. Note that the A^{10+} peak coincides with C^{3+} and O^{4+}, and is therefore not marked.

Figure 13. Quantity of charge expelled versus the length of the confinement region.

Figure 14. a) Quantity of charge expelled as a function of electron gun voltage.

b) Quantity of charge expelled versus magnetic field strength. The solid lines indicate the predicted charge for a beam

loading (ion charge divided by beam charge) of 30% and 33%, respectively.

Figure 15. Extracted ion pulse versus time. The pulse is stretched from its "natural" width of 30 μs to 5 ms.

Figure 16. Ten shot overlay of the total ion charge expelled and the time of flight charge state spectrum, showing reproducibility. (The gating pulse is shown inverted in this oscillogram.)

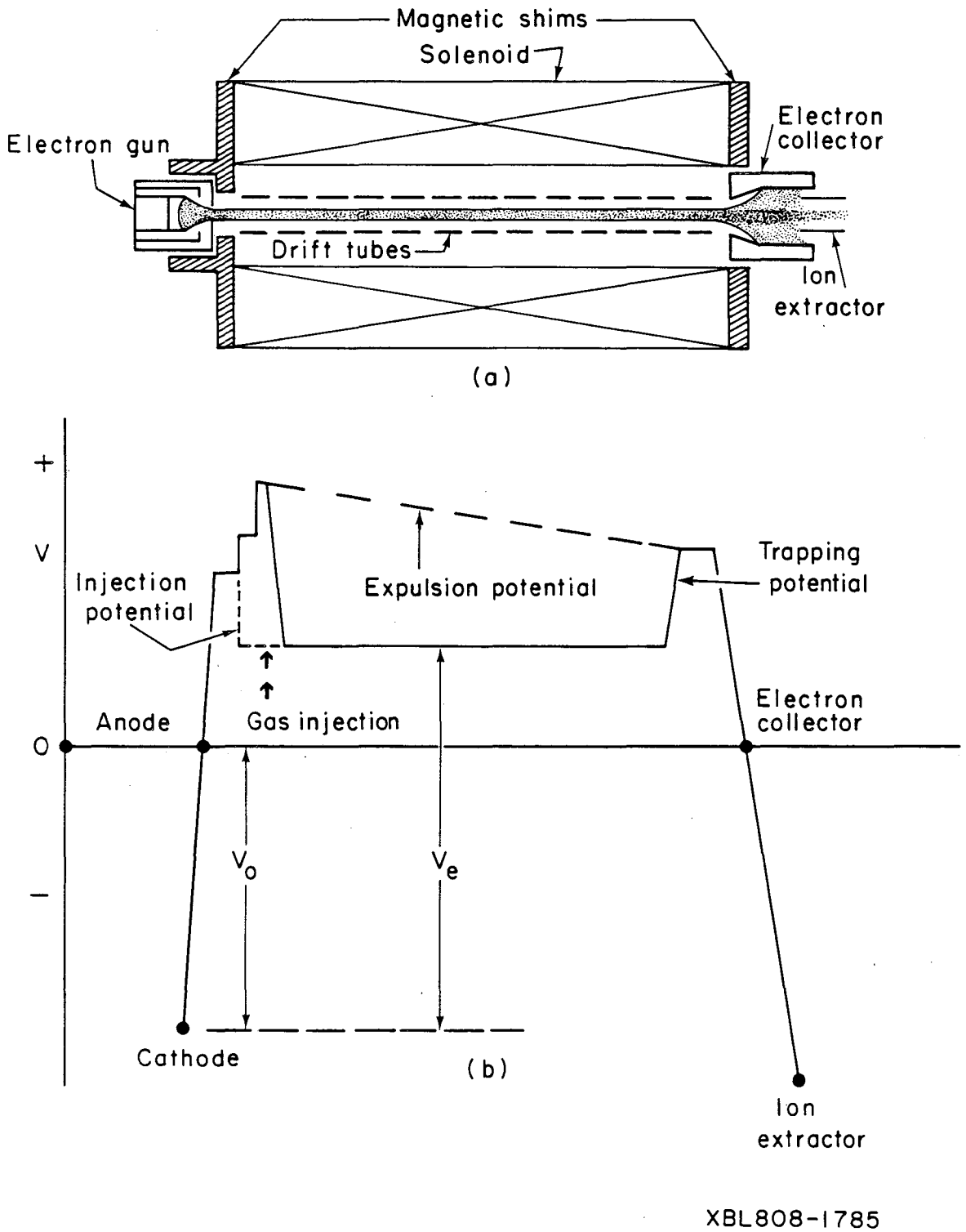
Magnetic shims
Solenoid
Electron gun
Electron collector
Drift tubes
Ion extractor
(a)
+
V
Injection potential
Expulsion potential
Trapping potential
Anode
Gas injection
Electron collector
0
V_o
V_e
−
Cathode
(b)
Ion extractor
XBL808-1785

Figure 1

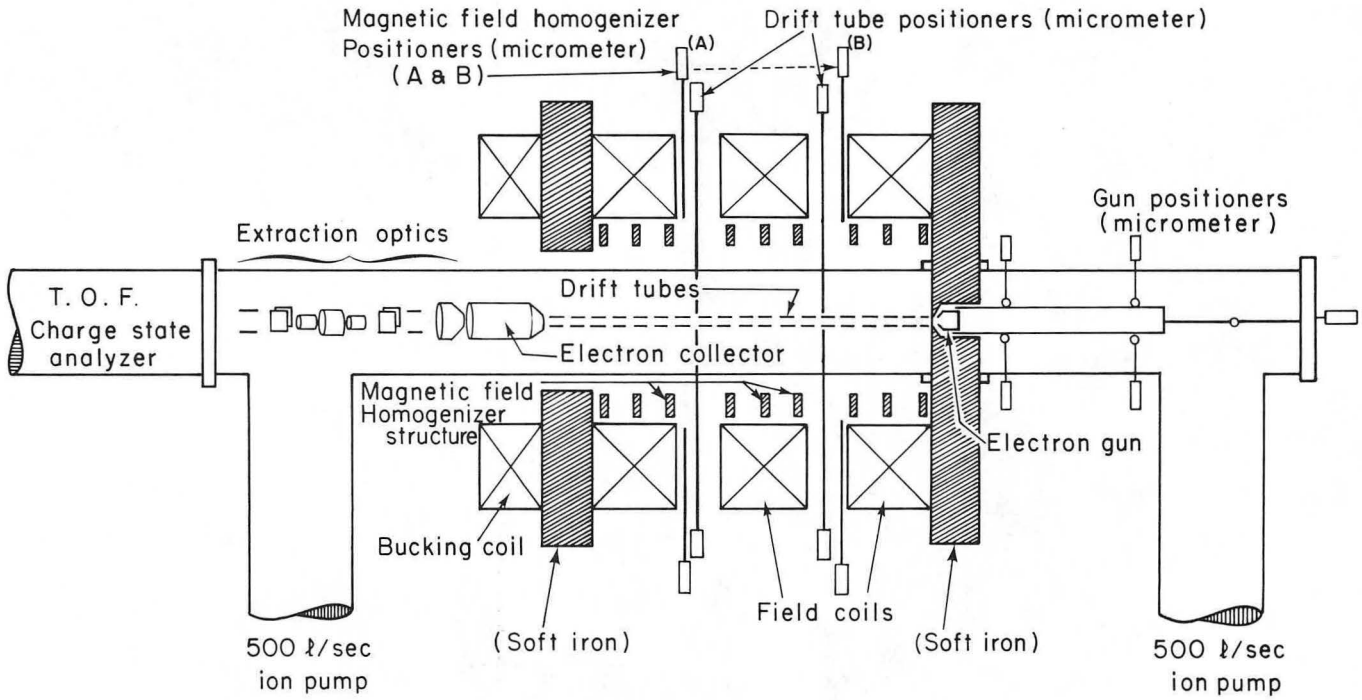

XBL808-1786

Figure 2
Page 27

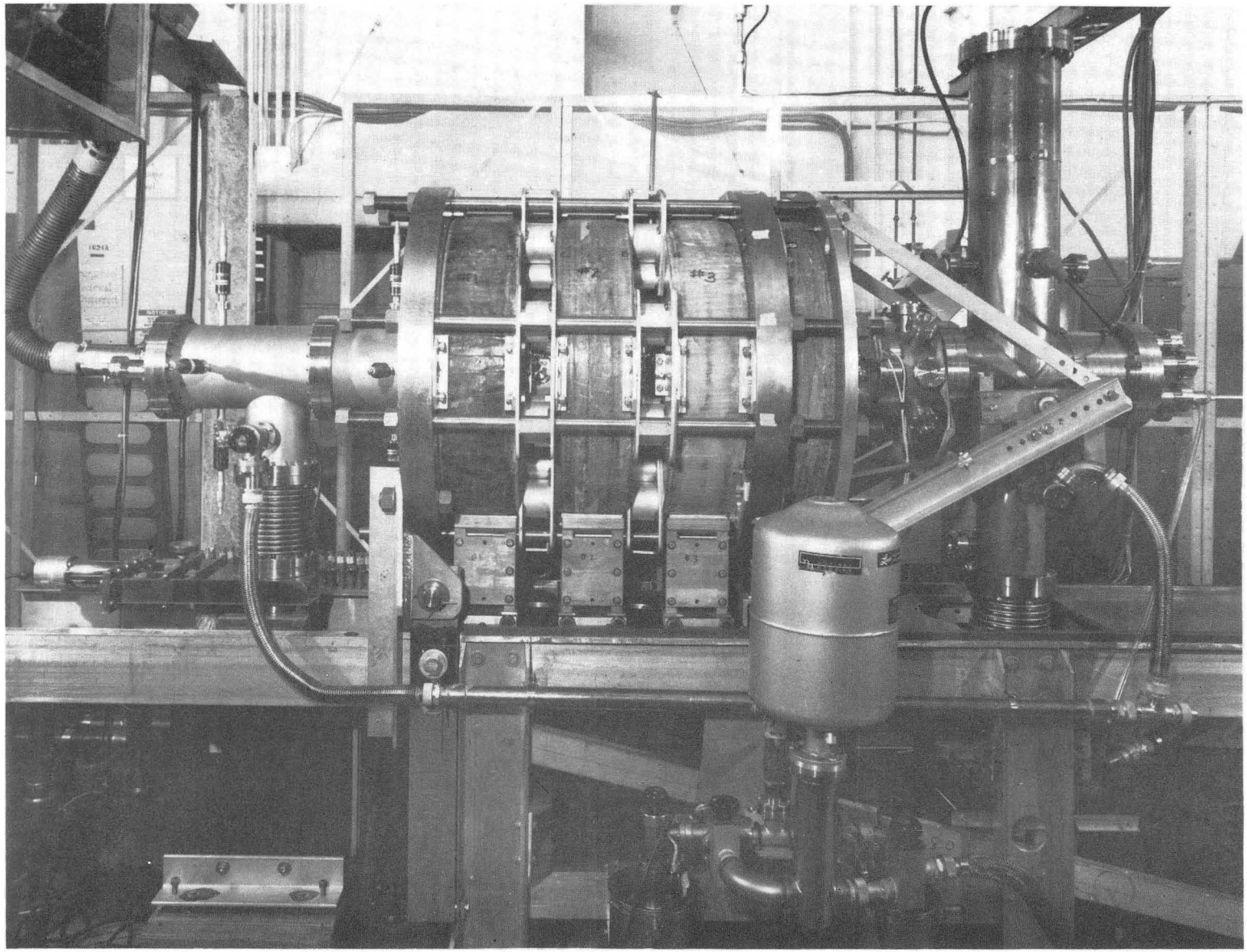

Figure 3 CBB 800-12339

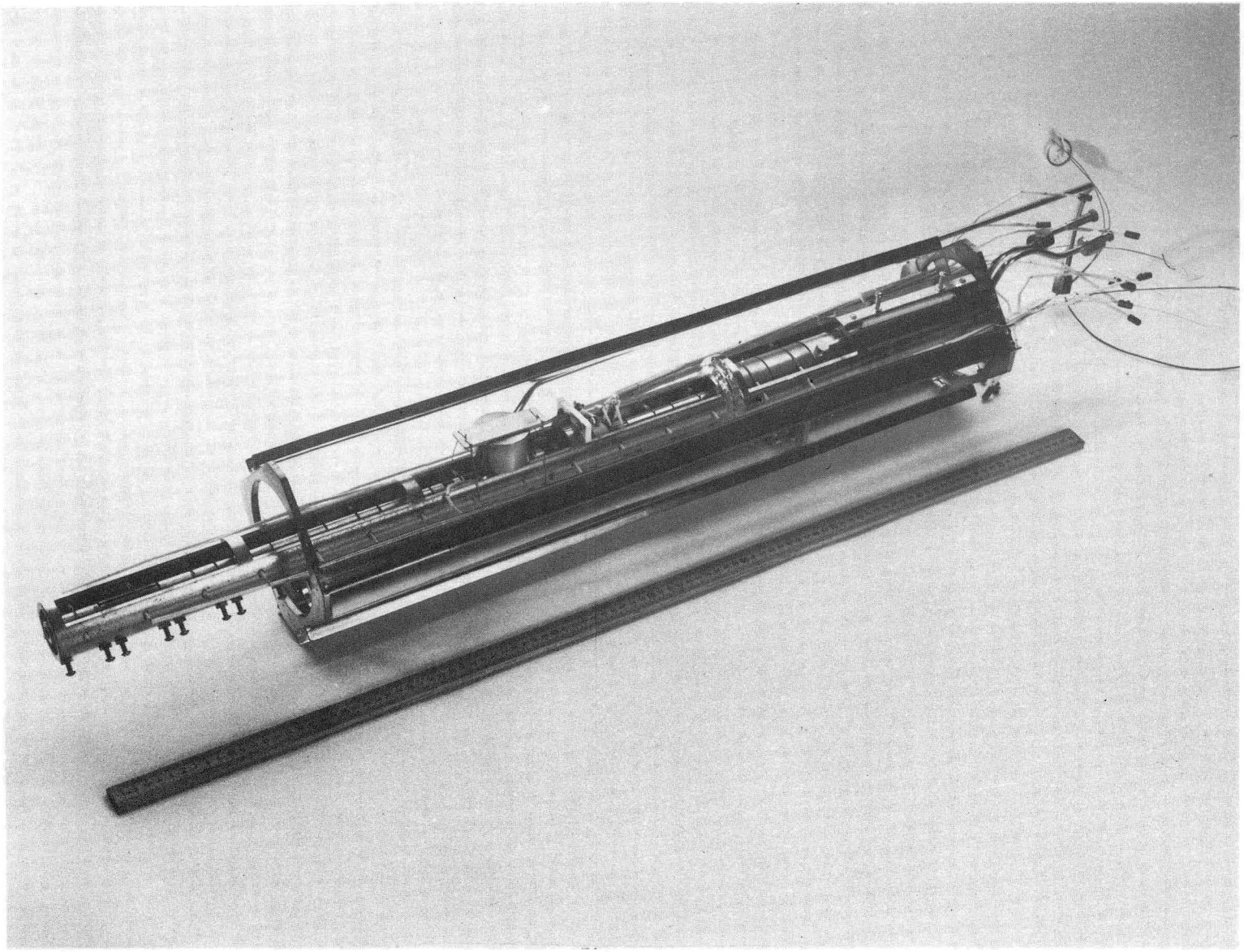

Figure 4

CBB 827-6355

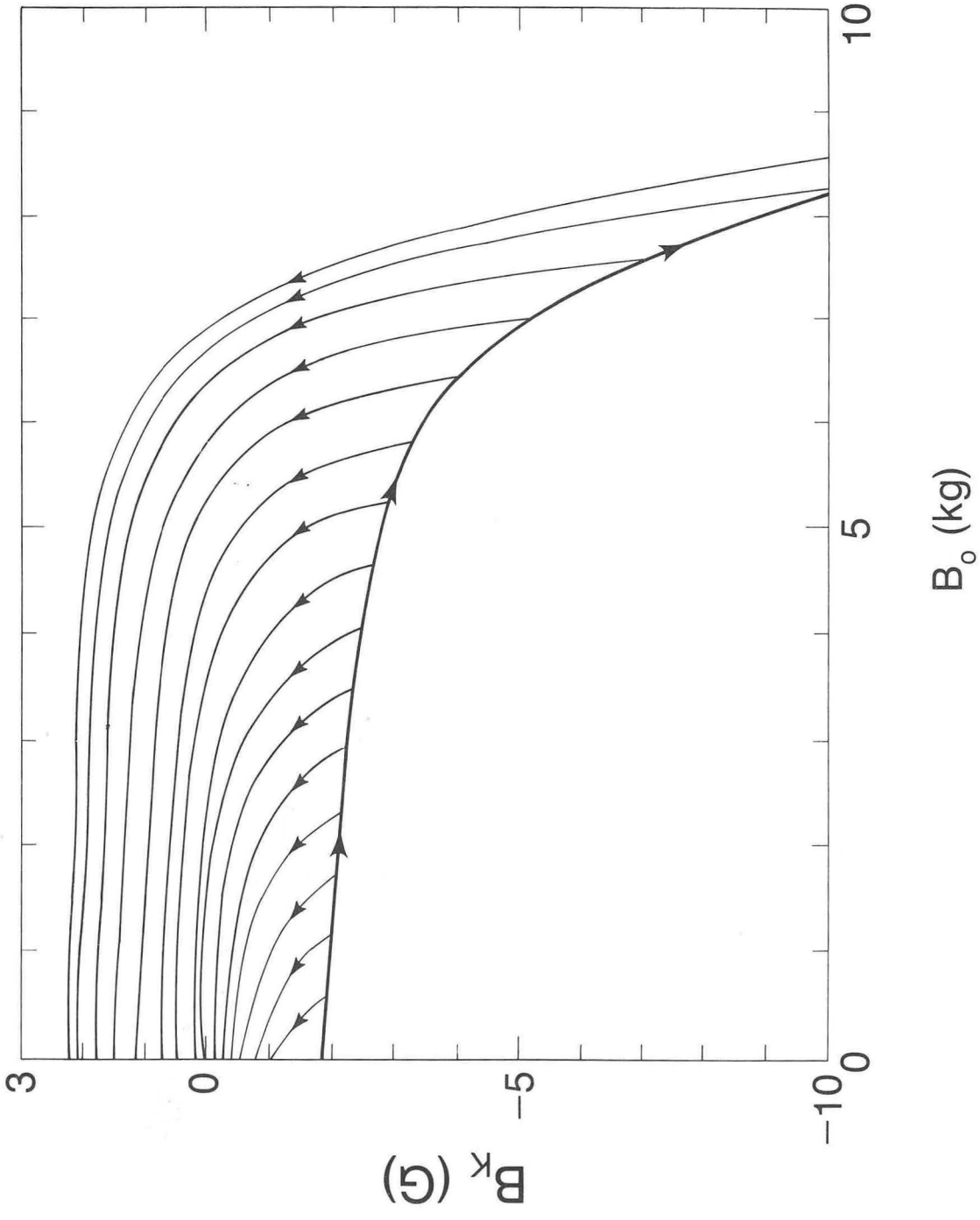

XBL 838-3015

Figure 5

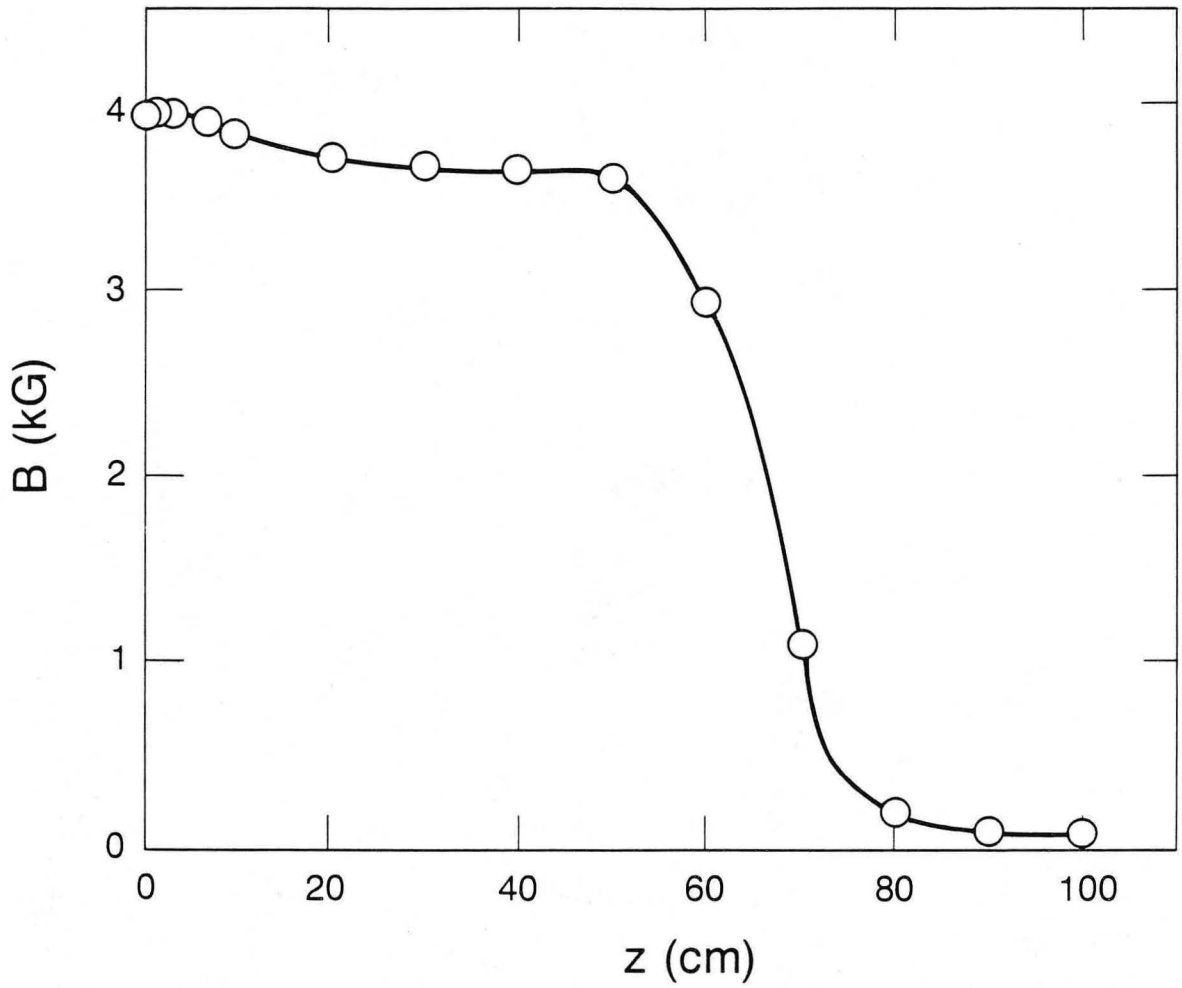

XBL 838-3019

Figure 6

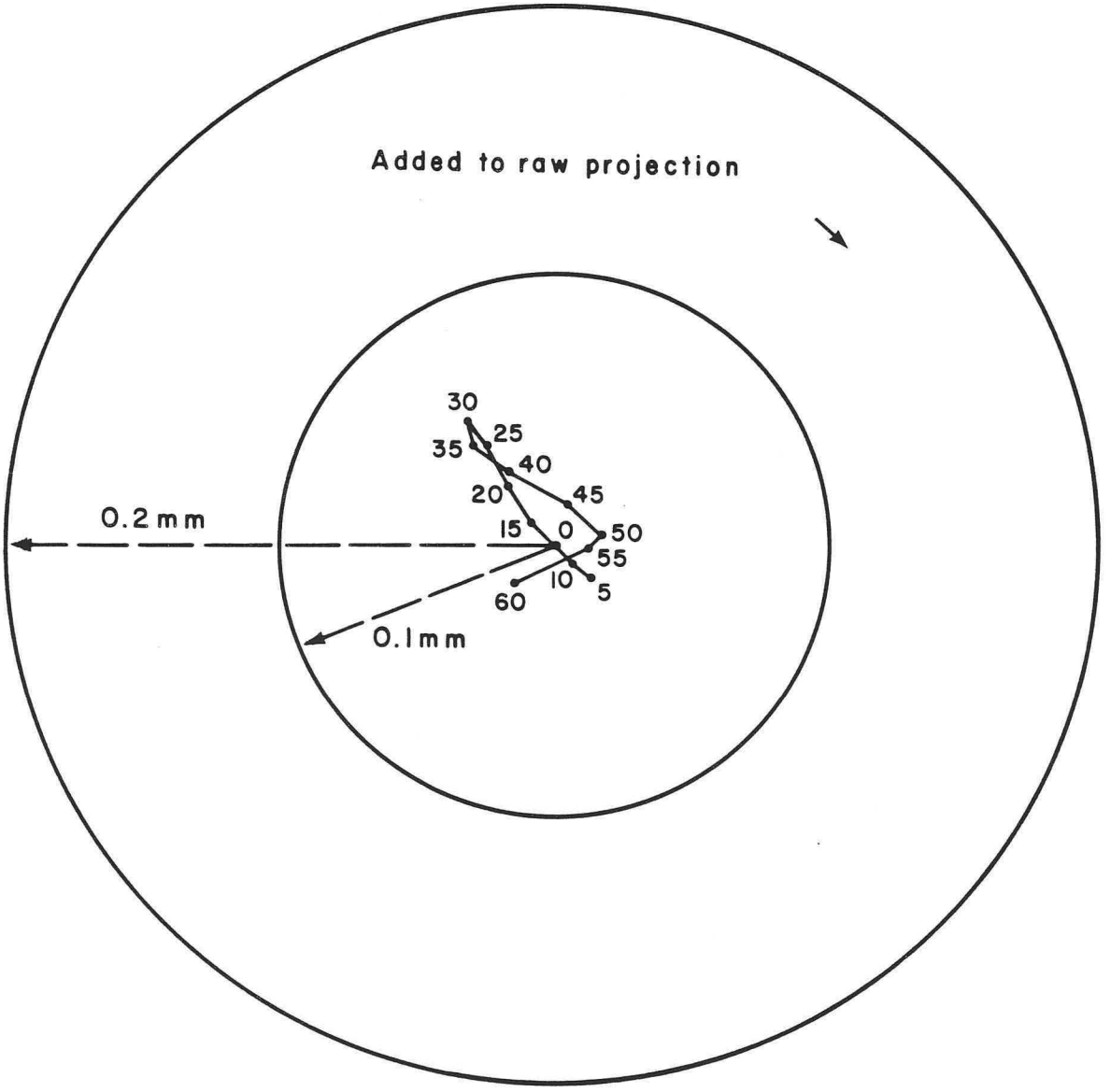

XBL 814-759

Figure 7a

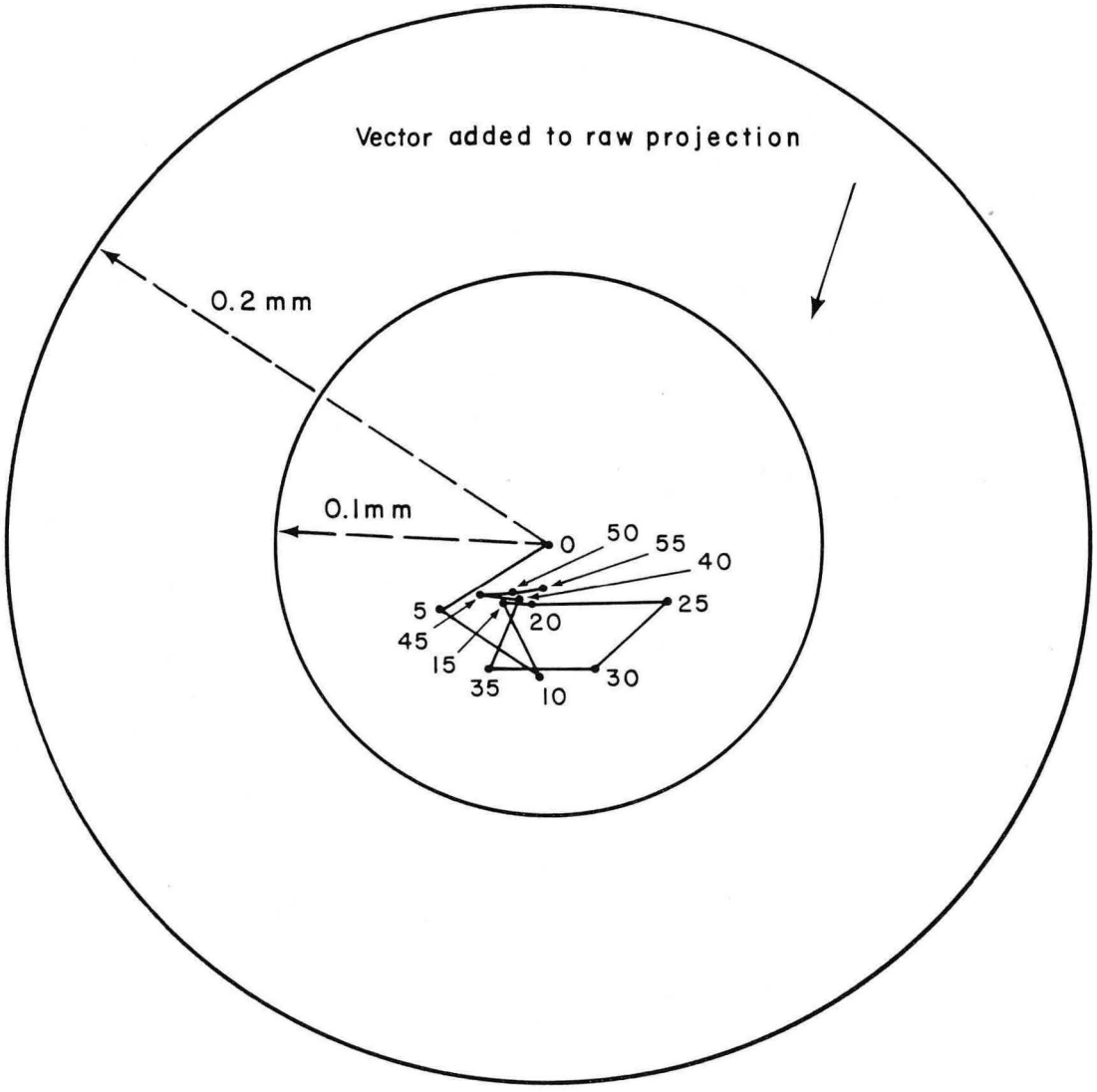

XBL 814-758

Figure 7b

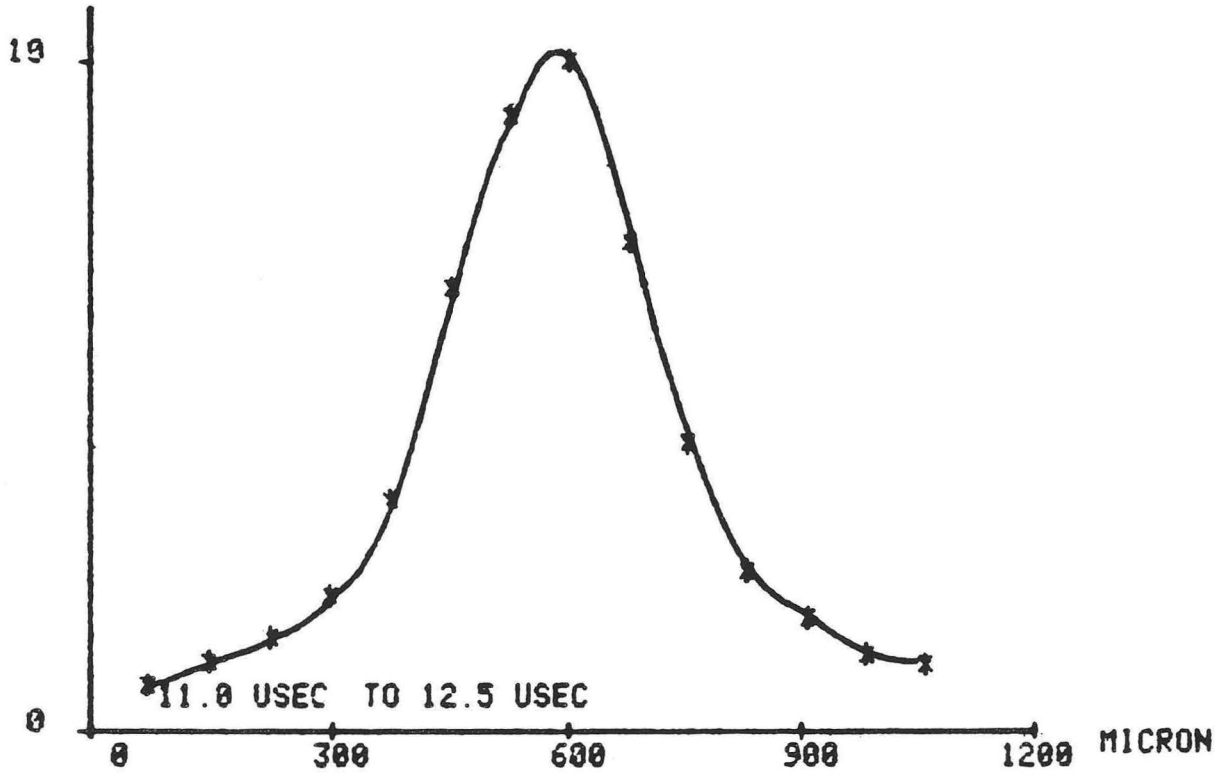

XBL 815-9493

Figure 8a

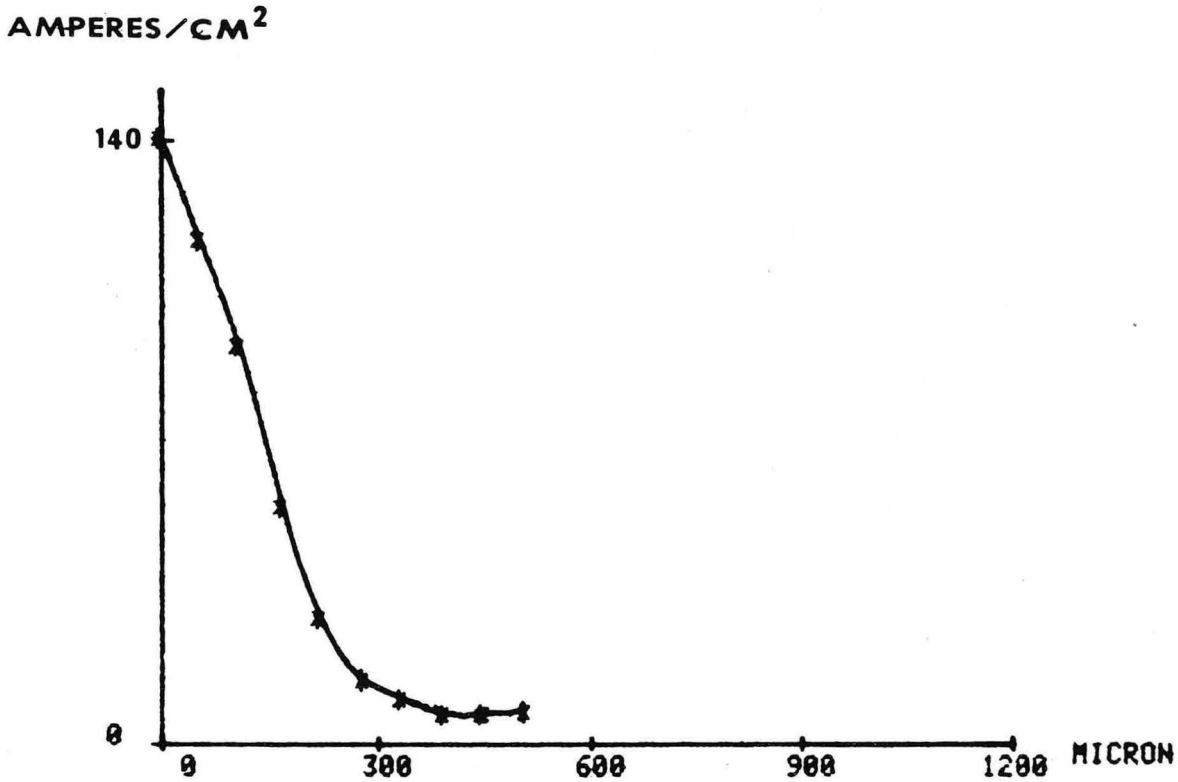

XBL 815-9521

Figure 8b

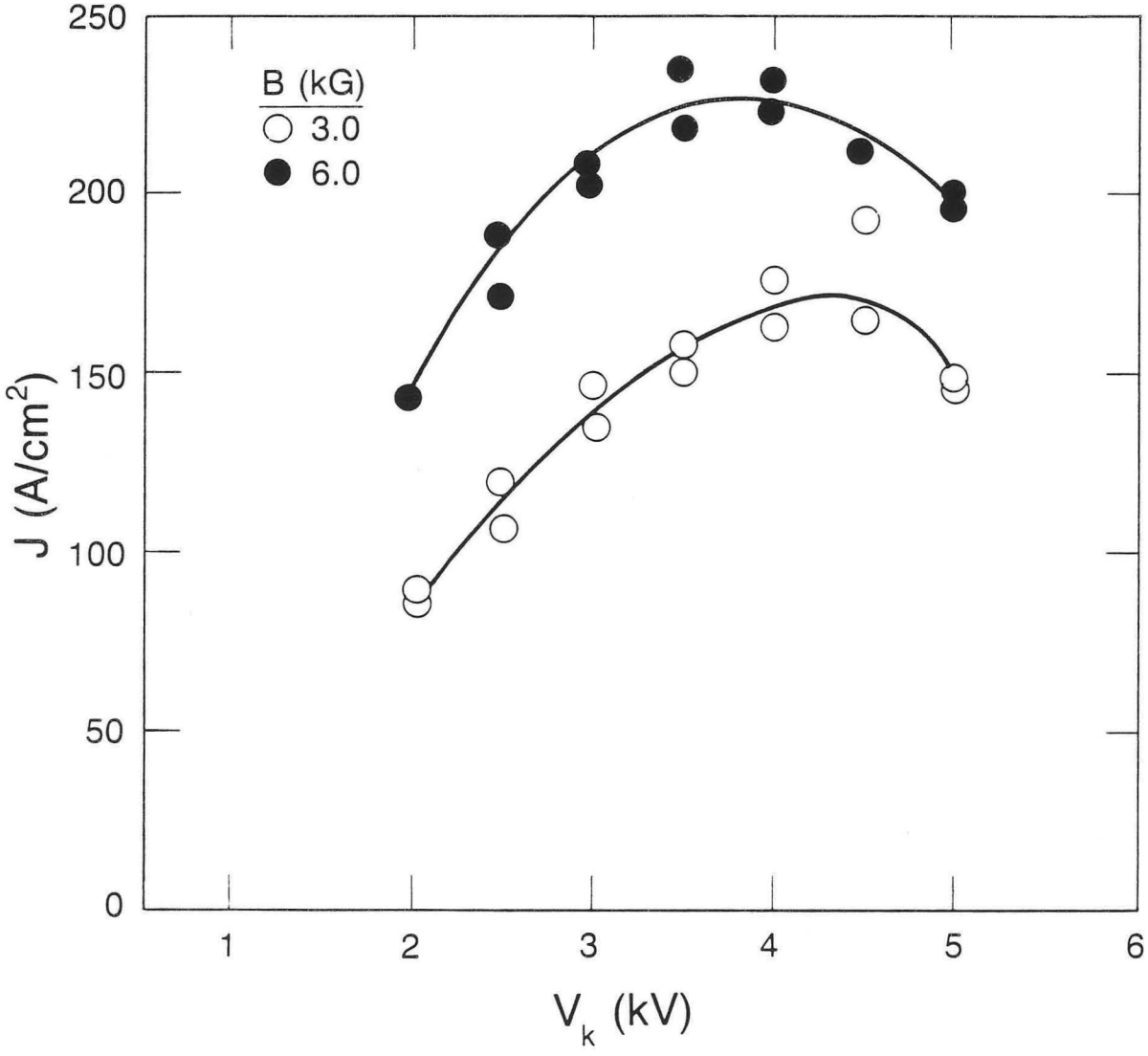

XBL 838-3020

Figure 9a

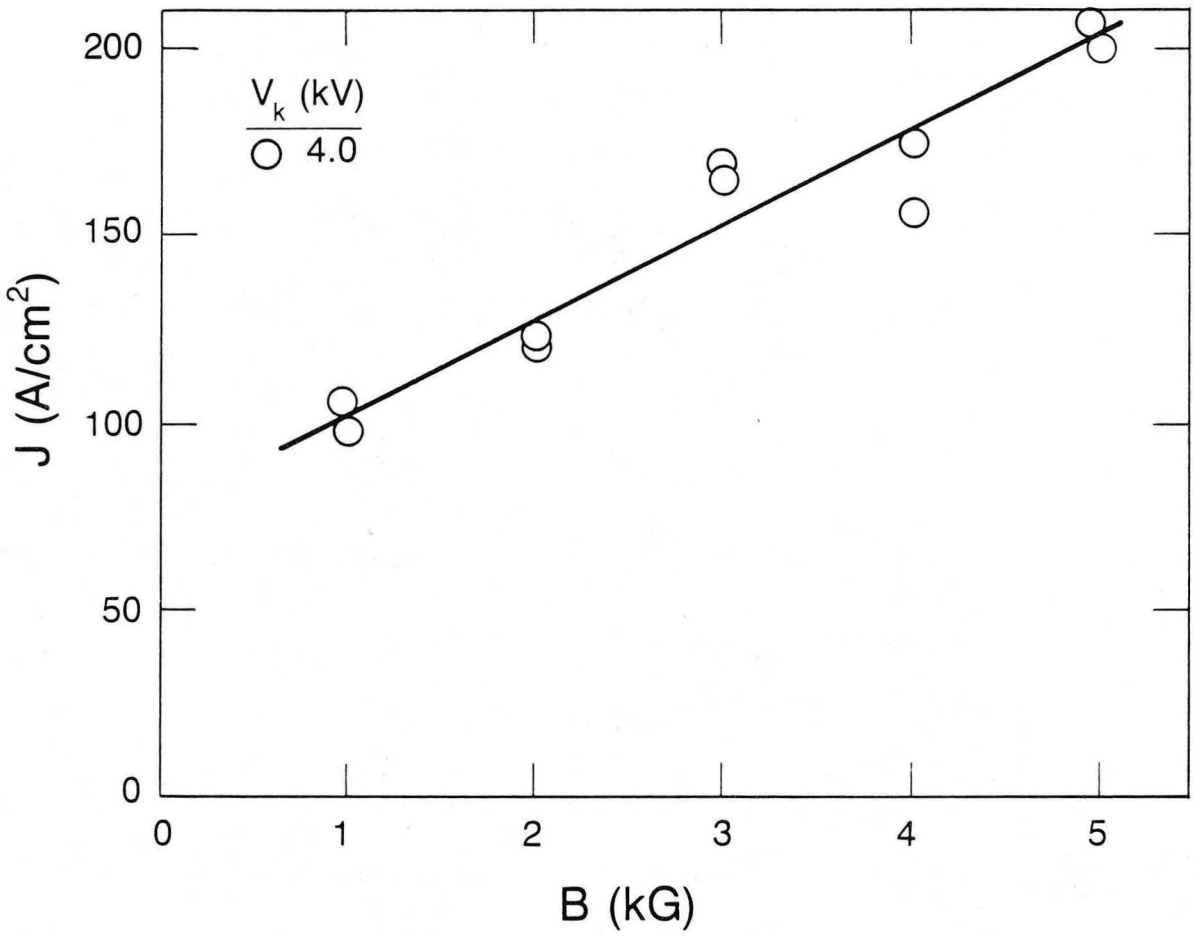

XBL 838-3021

Figure 9b

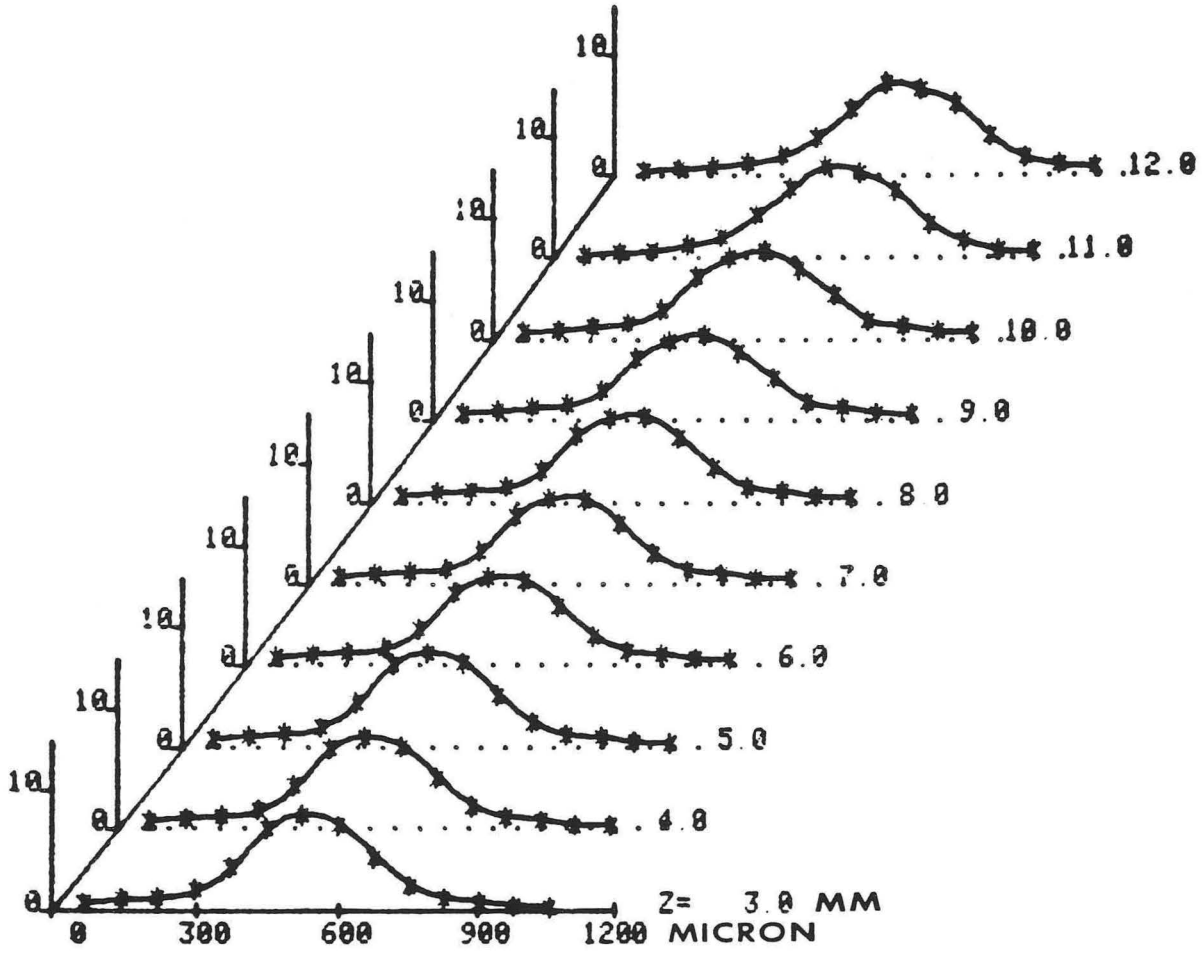

XBL 815-9492

Figure 10

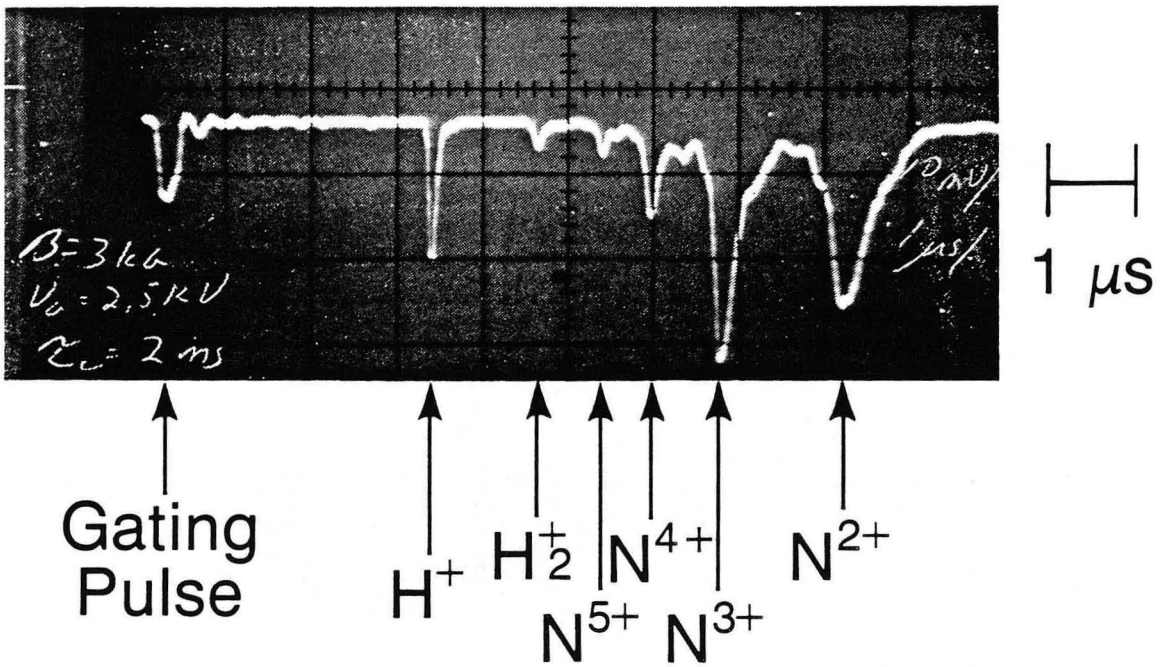

XBL 838-3001

Figure 11

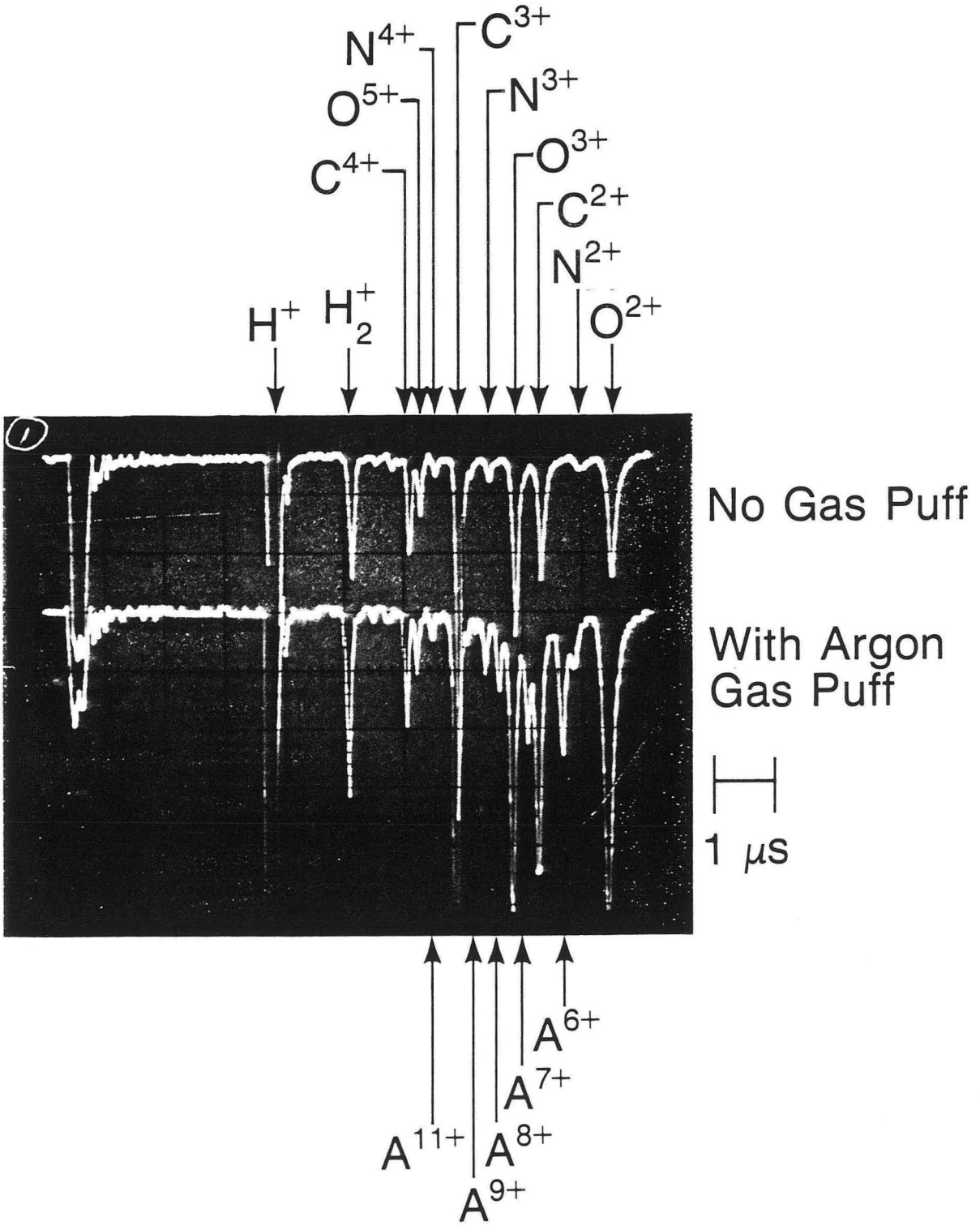

XBL 838-3002

Figure 12

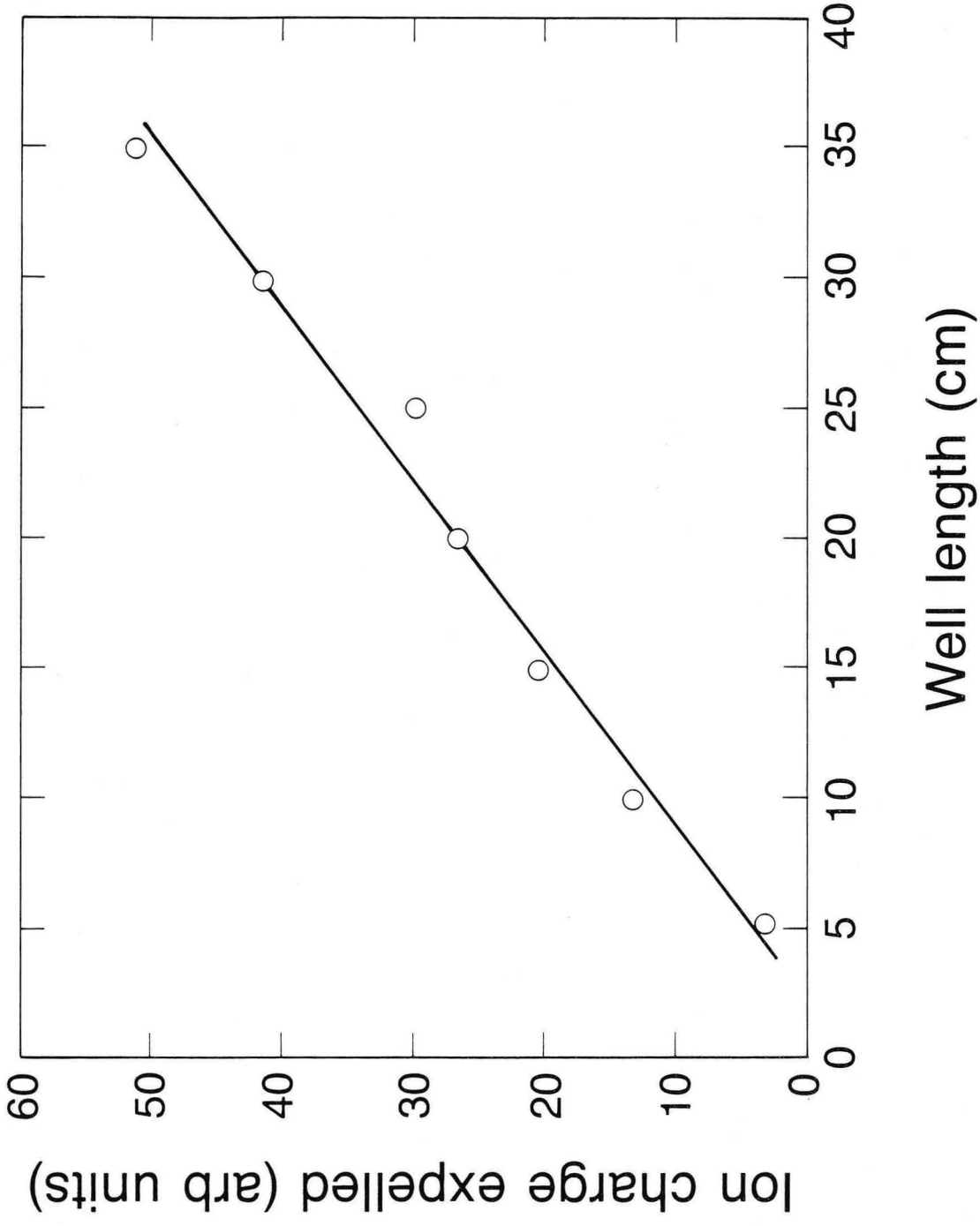

XBL 838-3022

Figure 13

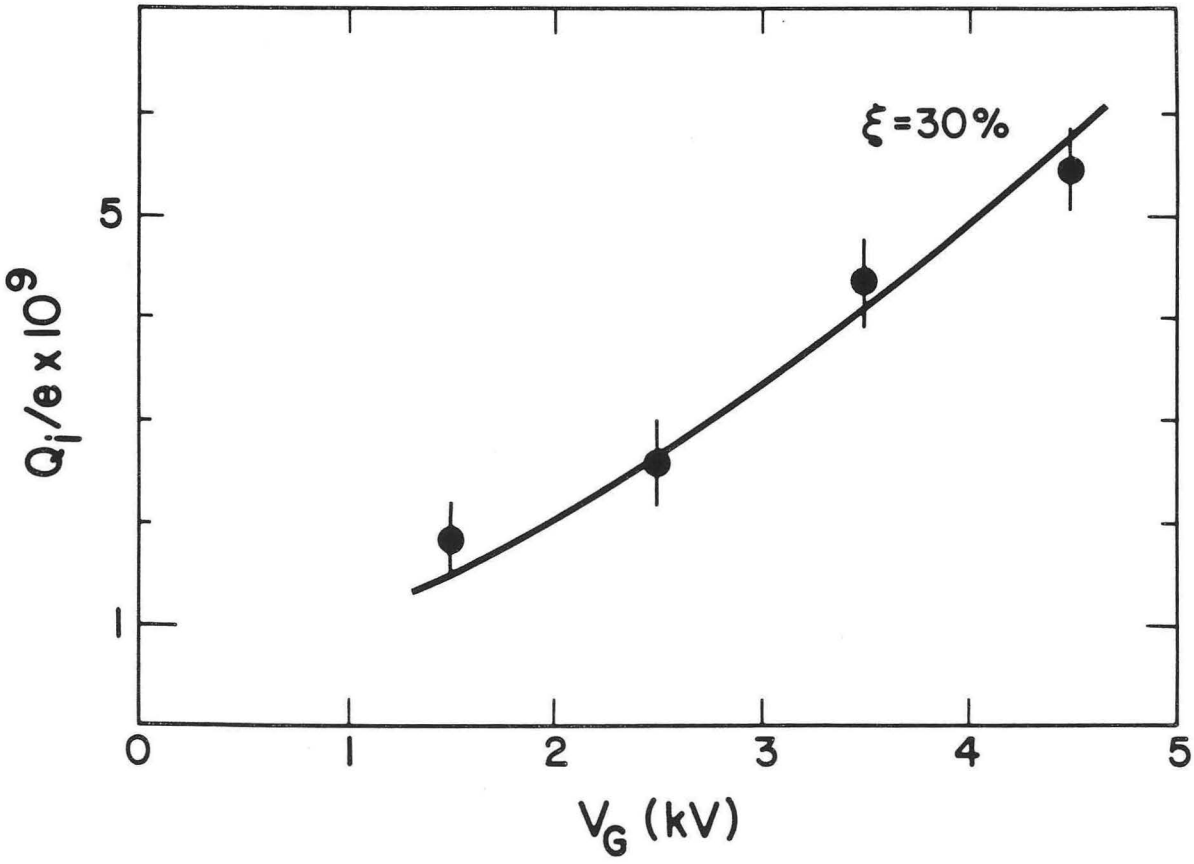

XBL 8210-4774

Figure 14a

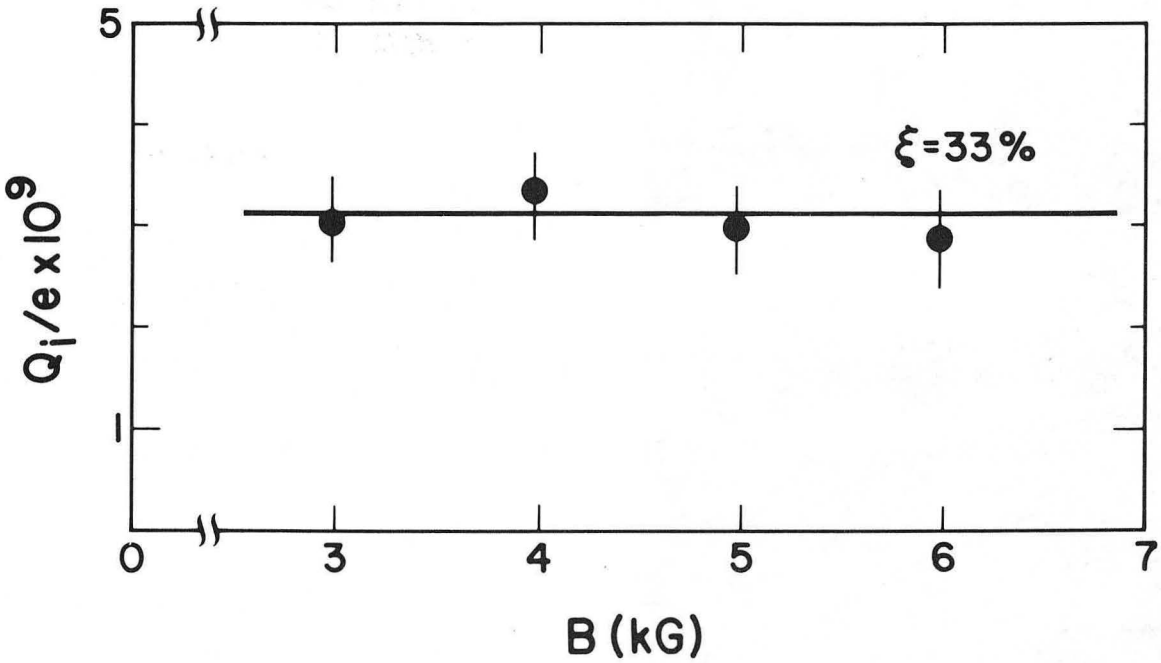

XBL 8210-4772

Figure 14b

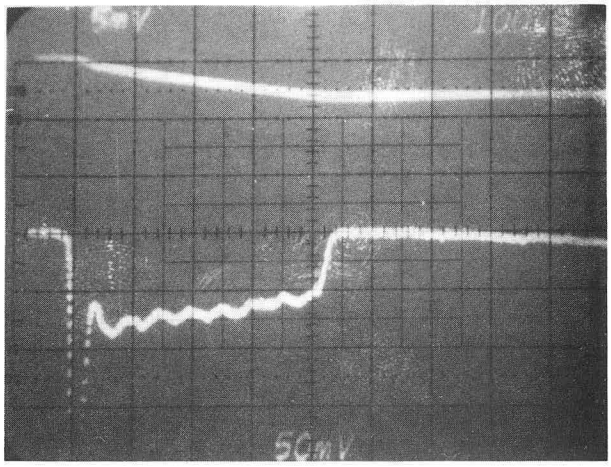

Q(t)

FARADAY CUP
SIGNAL, I(t)

t ~ 400 μsec

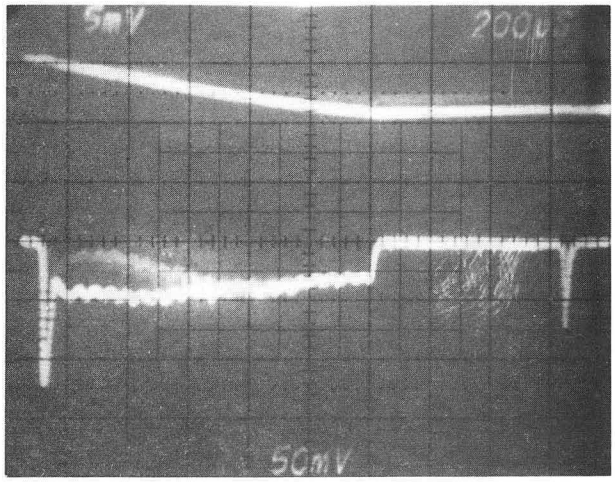

t ~ 1 msec

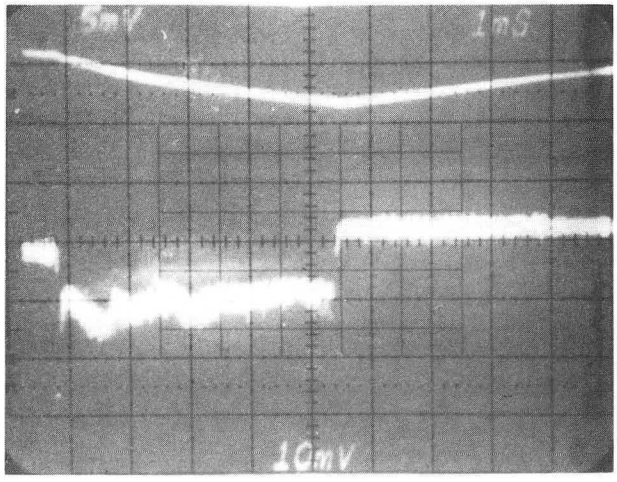

t ~ 5 msec

Figure 15

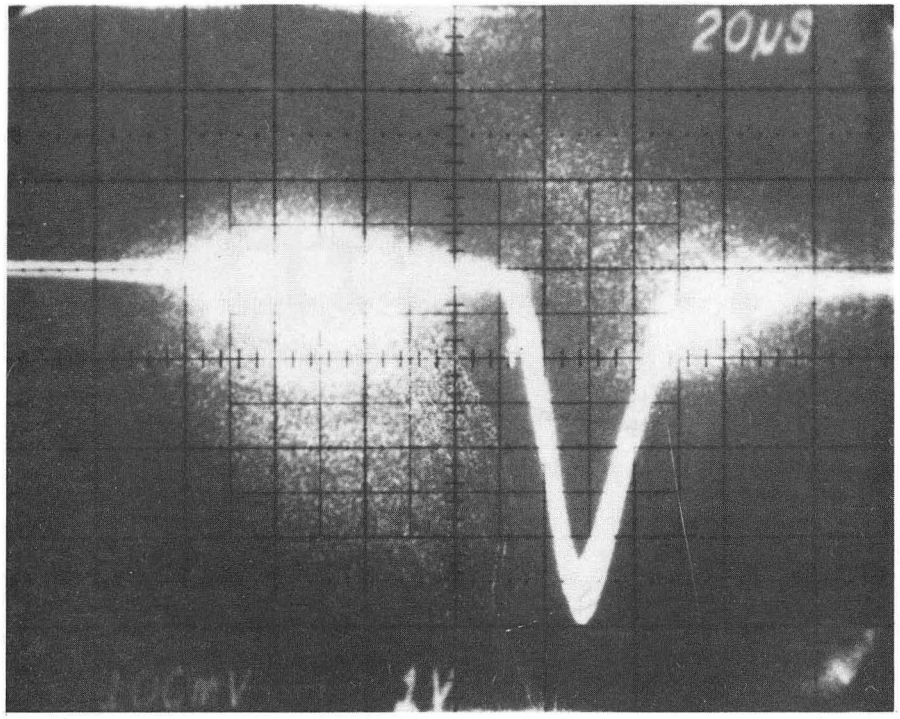

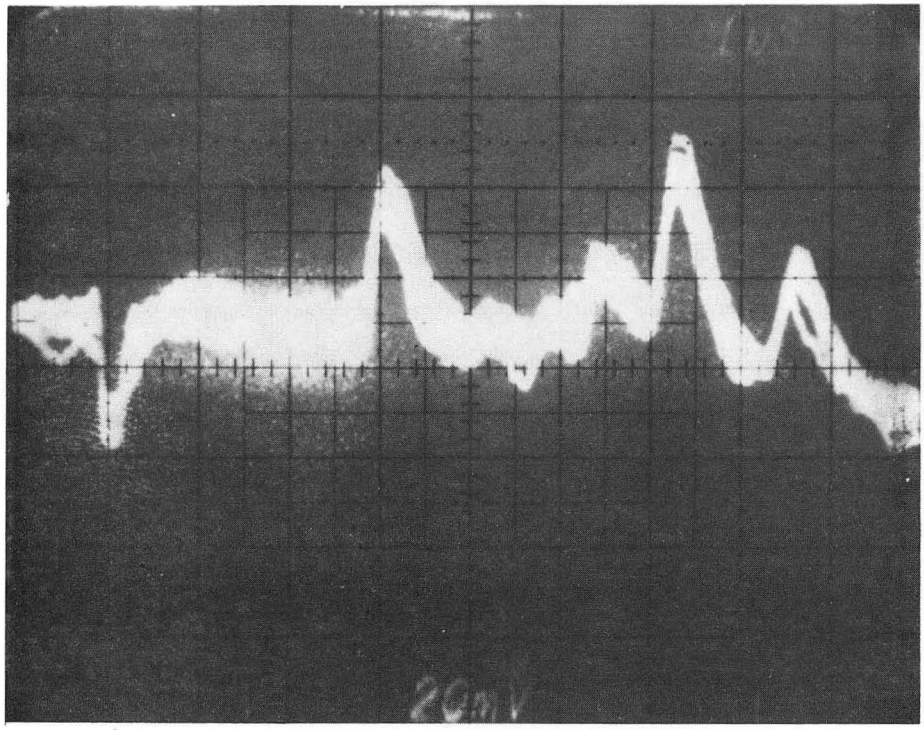

Figure 16

This report was done with support from the Department of Energy. Any conclusions or opinions expressed in this report represent solely those of the author(s) and not necessarily those of The Regents of the University of California, the Lawrence Berkeley Laboratory or the Department of Energy.

Reference to a company or product name does not imply approval or recommendation of the product by the University of California or the U.S. Department of Energy to the exclusion of others that may be suitable.

TECHNICAL INFORMATION DEPARTMENT
LAWRENCE BERKELEY LABORATORY
UNIVERSITY OF CALIFORNIA
BERKELEY, CALIFORNIA 94720